15 Agricultural Remote Sensing using Radio-Controlled Model Aircraft

E. Raymond Hunt Jr., Craig S. T. Daughtry, Charles L. Walthall, James E. McMurtrey III, and Wayne P. Dulaney

USDA-ARS Hydrology and Remote Sensing Laboratory
Beltsville, Maryland

ABSTRACT

Radio-controlled model aircraft may be useful as a platform for agricultural remote sensing because the data have high spatial resolution and the aircraft can be flown over individual fields in a timely manner. As a test of concept, an automatic 35-mm camera with color-infrared film was mounted on a fixed-wing radio-controlled model aircraft and flown over a field of corn (*Zea mays* L.) with three different planting dates and with various levels of applied N. The Normalized Difference Vegetation Index (NDVI) was calculated from scanned images of the photographic transparencies. Images of the same field were acquired on two dates using the AISA sensor, flown on-board a conventional aircraft. The color-infrared NDVI was linearly related to that obtained by the AISA sensor, NDVI from neither sensor was related to the level of applied N. Cameras on-board radio-controlled model aircraft can provide useful data on plant growth and cover; the low cost of the system may offset some of the limitations with this technology.

There is a strong potential for application of remotely sensed imagery in precision agriculture (Lu et al., 1997; Moran et al., 1997; Pierce & Nowak, 1999). Remotely sensed data may be combined with other data in a geographic information system and used to control applications of fertilizer and other treatments based on the position in a field as determined by a global positioning system (GPS). Some satellites that provide low-cost imagery, such as Landsat, may have limitations for precision agriculture primarily because of sensor- and platform-specific resolutions (Moran et al., 1997). What is needed is a means of acquiring high-resolution imagery at low cost.

Selection of a specific platform for remote sensing is a compromise among spatial resolution, spectral resolution, radiometric resolution, temporal resolution, and cost. Spatial resolution is the pixel size; imagery with small pixel size generally cover small areas on the ground, so the image has a large map scale. Spectral resolution is the number of wavelength bands on the sensor, and whether each of

 Digital Imaging and Spectral Techniques: Applications to Precision Agriculture and Crop Physiology. ASA Special Publication no. 66.

these bands cover a small or a large wavelength interval (narrow or wide bands, respectively). Radiometric resolution is the number of bits for each pixel at each band; a larger number of bits is generally associated greater accuracy and is generally less likely to be saturated by the incoming signal. Temporal resolution is the repeat frequency of the platform; aircraft can fly often whereas satellites, such as Landsat, fly over at periodic intervals and acquire imagery whether or not it is cloudy. Furthermore, there is a delay between image acquisition and delivery to the user. Aircraft and satellite platforms and sensors can provide the spatial and temporal resolution required for precision agriculture; however, these data are more expensive.

Quilter and Anderson (2000) suggested that fixed-wing radio-controlled model aircraft with camera sensors can provide a low-cost method of obtaining aerial photographs. Camera sensors can provide useful data, particularly for nutrient management, when flown in regular airplanes or helicopters (Blackmer et al., 1996; Scharf & Lory, 2002). Flying radio-controlled model aircraft (RCMA) is a hobby enjoyed by people all over the world, and in response to the large demand, there have been many technological advances in engines, materials, and controllers. There are several private companies and research groups using RCMA for remote sensing platforms. The results from these studies have not yet been published.

The objective of this study was to explore the idea of using fixed-wing RCMA for remote sensing, as a potential tool for precision agriculture. To accomplish this objective we compared the RCMA imagery with an advanced airborne imaging sensor, in order to assess the strengths and weaknesses of RCMA imagery.

MATERIALS AND METHODS

Experimental Design and Ground Data Collection

The expense of multiple aircraft overflights was reduced by having three planting dates of corn (Pioneer hybrid 33K78) in Field 5-21 at the Beltsville Agricultural Research Center: an early planting on 2 May, a middle planting date on 31 May, and a late planting date on 15 June 2001 (Plate 15–1). Starter N (20 kg N ha^{-1}) was applied at planting to the whole field. For each planting date, 11 plots of 30.5 m by 36.6 m (48 rows) were established (except the third plot that was 36.6 by 36.6 m to avoid a bare spot). The N levels were 0, 25, 50, 100, and 150% of 145 kg N ha^{-1}, applied as sidedress (Plate 15–1). The plots with the same planting date were randomly assigned a N treatment, such that there were two replicates of each N level, and three replicates of the 0% level.

Crows removed some corn seedlings so the plant density varied considerably among plots. Density was determined by counting the number of plants in 6 rows, which were evenly spaced across the plot. One area (in plot 3, early planting date) had very low initial density of seedlings, so all corn seedlings were removed and the area was kept weed-free and bare for image calibration (Plate 15–1). The reflectances of the bare plot were measured using a Fieldspec Pro FR spectroradiometer (Analytical Spectral Devices, Boulder, CO)[1] calibrated to a Spectralon white panel.

[1] Trade names and companies are mentioned for information only, and do not indicate endorsement by USDA.

The corn hybrid was a 108-d variety. In late August 2001, the plants for all three planting dates were between the silking and dent reproductive stages, during which the number of leaves does not vary much (Ritchie et al., 1993).

Radio-Controlled Model Aircraft

A "Ready-to-fly" fixed-wing trainer aircraft (Hanger 9 Xtra Easy, Horizon Hobby, Champaign, IL) was assembled from a kit with an MDS 0.41 cubic inch engine and a JR XF421EX five-channel radio transmitter. An Olympus XB41AF automatic 35-mm camera was mounted on the aircraft fuselage. The camera has a lens focal length of 28 mm (wide angle), in order to obtain large areas of the field in a single photograph. The camera shutter button was operated using a servo motor connected to the fifth channel of the radio transmitter, so that photographs were taken under the control of the pilot. We timed how fast the camera could take photographs, and calculated from optical laws that taking one photograph per second along a flight line at 150 m altitude with an air speed of 50 km h^{-1} results in a photograph overlap of about 50%, allowing for easier geographic registration of multiple images.

The film used was Ektachrome Professional Infrared EIR slide film (Kodak, Rochester, NY), with a film speed of ISO 200. The automatic camera above was selected because more expensive automatic cameras use internal near-infrared sensors, which may expose the color-infrared film. The front of the camera was covered with two sheets of yellow cellophane to serve, first as a yellow filter required for the film, and second to protect the camera from the engine exhaust. The default film speed of the camera was ISO 100, so the film was overexposed, which was compensated somewhat by underdevelopment with the E6 process.

In a separate experiment, we determined the effective spatial resolving power of the camera/film system. Targets were constructed of alternating black and white stripes that were 2.5 cm wide. These targets were placed at different distances from the camera; when the targets were sufficiently far from the camera, the black and white stripes appear to be gray on the photographic transparency. The farthest distance that the black and white stripes were still distinct was 17 m, resulting in an angle of 1.5 mrad (0.09°). This translates to a 23-cm pixel at an altitude of 150 m; under normal flight conditions it is difficult to measure the actual altitude of the model aircraft.

Image Data Analysis

AISA images (Specim, Spectral Imaging Ltd, Oulu, Finland; www.specim.fi) were acquired from a private company (3Di LLC, Easton, MD) on two dates, 7 July and 22 August, 2001 over the corn field in Plate 15–1. The pixel size was 2.5 m. These data were georeferenced with a differential global positioning system and inertial guidance unit to an accuracy of 5 m. The number of bands on the AISA sensor are user selectable; the data acquired had 34 narrow bands from 400 to 900 nm wavelength. The radiance values for each band were corrected to reflectance with an uplooking radiation sensor.

Two vegetation indices were calculated from the plot average reflectances. First, the Normalized Difference Vegetation Index (NDVI) was calculated:

$$\text{NDVI} = (R_{806} - R_{681})/(R_{806} + R_{681}) \quad [1]$$

where R_{806} is the reflectance in the near infrared and R_{681} is the reflectance in the red. The Modified Chlorophyll Absorptance Reflectance Index (MCARI) was calculated:

$$\text{MCARI} = [(R_{698} - R_{681}) - 0.2(R_{698} - R_{549})](R_{698}/R_{681}) \quad [2]$$

where R_{698} and R_{549} are two wavelengths used to normalize the chlorophyll absorption feature (Kim, 1994; Daughtry et al., 2000).

Color-infrared transparencies from the model aircraft were acquired on 29 Aug. 2001. As the authors could not fly the model aircraft, we initially used volunteers from the Academy of Model Aeronautics Goddard Model Aircraft Club. Later we hired a qualified student to be the pilot, and were able to acquire RCMA images of the field.

The color-infrared transparencies were scanned at 1600 lines per inch. The colors of the scanned images were separated to obtain the near infrared, red and green bands, and NDVI was calculated from the red and near-infrared bands. The scanned images were registered to the AISA image with an average accuracy of 5.5 m. All of the pixels in a plot were averaged together to obtain the mean vegetation index of each plot in the AISA and RCMA images.

RESULTS AND DISCUSSION

Selection of the RCMA platform depends on numerous factors (Table 15–1); there are positive and negative features of blimp, fixed wing, and helicopter model aircraft. Generally, the easiest platform to use are blimps, because helium provides the lift. Fixed wing aircraft are easier to fly than helicopters, but helicopters can take off and land vertically whereas fixed wing aircraft require grassy strips or runways for takeoff and landing (Table 15–1). All model aircraft are susceptible to wind; fixed wing aircraft can operate with moderate amounts of wind. Also, all model aircraft are susceptible to flight failure due to radio transmitter/receiver problems, turbulence, engine problems, or simply running out of fuel. With flight failure common, maintenance of control is important to prevent loss of the aircraft and sensor. Fixed wing aircraft can be glided to a landing; helicopter auto-rotation is a difficult ma-

Table 15–1. Characteristics of different radio-controlled model aircraft.

Platform	Ease of use	Takeoff/ landing	Wind conditions	Distance covered	Failure response
Blimp	Easy	Vertical	Very light	Least	Sink
Fixed wing	Moderate	Runway	Moderate	Most	Glide
Helicopter	Hard	Vertical	Light	Middle	Auto-rotation

neuver that requires considerable expertise (Table 15–1). Since the aircraft are piloted from the ground, the user must keep in eye contact, thereby restricting RCMA imagery to about one field per flight.

Seedlings were visible in the 7 July AISA image for the corn planted on the early and middle planting dates, but seedlings were not yet visible for corn planted on the late planting date (Plate 15–2A). The image shows the large differences in plant density that were visible in the early planting date also were visible in the 22 August AISA image (Plate 15–2B).

For the 7 July AISA image, there was a strong correlation between NDVI and MCARI related to the differences in plant density (Fig. 15–1A; $R^2 = 0.84$, $P > 0.9999$); however, for the 22 August AISA image, there was negative relationship between NDVI and MCARI (Fig. 15–1A; $R^2 = 0.12$, $P = 0.96$). There was an inverse relationship between MCARI and the level of applied N (Fig. 15–1B; $R^2 = 0.55$, $P > 0.9999$). In the 7 July AISA image, NDVI was not related to the level of applied N ($R^2 = 0.01$, $P = 0.69$) or plant density ($R^2 = 0.02$, $P = 0.74$). Whereas for the 22 August AISA image, NDVI was not related to applied N ($R^2 = 0.10$, $P = 0.93$), but was correlated to plant density ($R^2 = 0.36$, $P = 0.999$). The bare plot (Plate 15–1) was not included in these analyses.

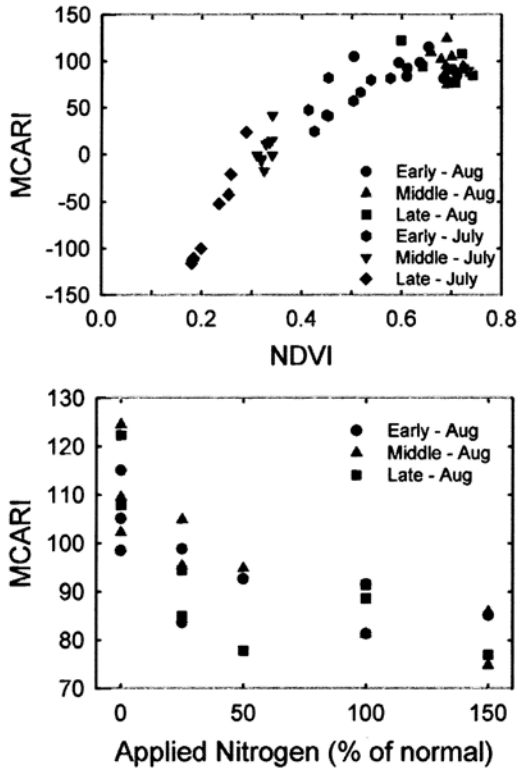

Fig. 15–1. Vegetation indices from the AISA sensor A. MCARI versus NDVI and B. MCARI versus applied nitrogen. Spectral resolution of the AISA sensor allows calculation of difference vegetation indices that were designed to be more sensitive to canopy chlorophyll concentration.

The differences in plant density from the color infrared RCMA images were much more apparent than in the AISA images (Plate 15–3). This is to be expected because of the much smaller pixel size of the RCMA color infrared image (0.2–0.4 m) compared with the AISA images (2.5 m). The center of the RCMA images was much brighter than the edges of the image due to angular differences between the sun, target, and sensor (canopy anisotropy), so it was difficult to mosaic several images together and obtain a satisfactory image of the entire field. Therefore, each image was analyzed separately. NDVI calculated from the RCMA image were not related to the level of applied N (Fig. 15–2A; $R^2 = 0.003$, $P = 0.62$). NDVI was correlated to plant density (Fig. 15–2B; $R^2 = 0.11$, $P = 0.97$), but the correlation was weak due to high NDVI at low plant density. Overall, the NDVI values were comparable between the RCMA image and the 22 August AISA image (Plate 15–4). Particularly, areas of low and high NDVI corresponded in each image. A scatterplot of NDVI's for the two images showed that there was some correlation (Fig. 15–3; $R^2 = 0.37$, $P = 0.999$), although there is a much greater range of NDVI from the RCMA images.

Reflectances and digital numbers of bare soil were compared using the data for the calibration plot (Fig. 15–4). The AISA and ground-measured reflectances

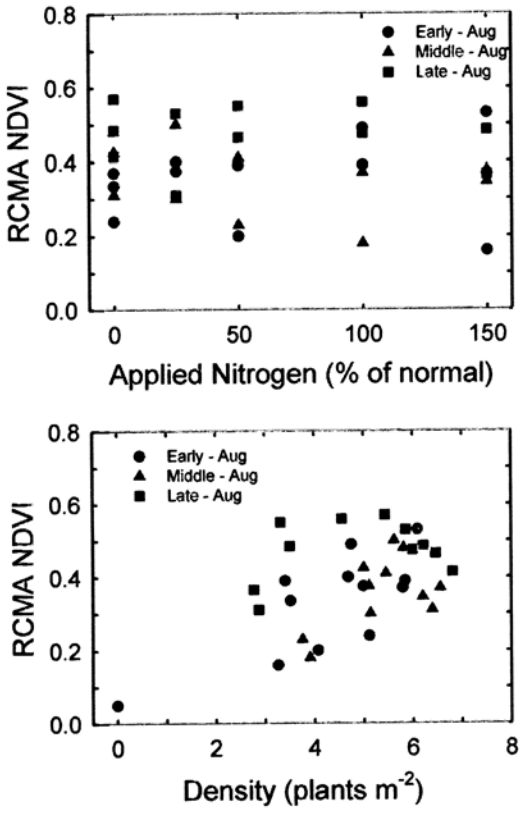

Fig. 15–2. NDVI from RCMA versus A. Levels of applied N and B. Plant density.

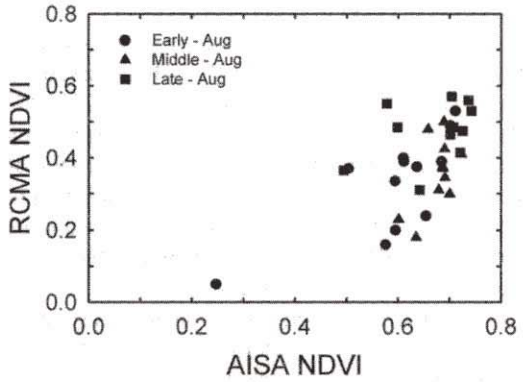

Fig. 15–3. Comparison of AISA NDVI and RCMA NDVI. Each point is the plot average.

were comparable, except for some residual atmospheric features in the AISA reflectance spectrum; however, the bands in these atmospheric features were not used for calculation of either NDVI or MCARI. The digital numbers of the RCMA image followed the trend in reflectances for the red and near-infrared bands, but not for the green band (Fig. 15–4). Hence, NDVI calculated from the RCMA images for this plot (Plate 15–4) were comparable. There may be a problem using the green band for remote sensing of nutrient stress, because the green digital number was greater than that of the red opposite of the trend for the reflectances (Fig. 15–4).

A general problem with all image data is canopy anisotropy (Walthall et al., 2000), which is the view-angle-dependent change in reflectance caused by non-Lambertian surfaces. The spectral reflectance will vary across the image of a uniform target because of different angles and directions between the sun, target, and sensor. This problem is particularly important in aerial photography when using wide angle lenses, such as those used with the cameras in this study, because part of the image will have a nadir view angle, and part of the image will have an oblique angle

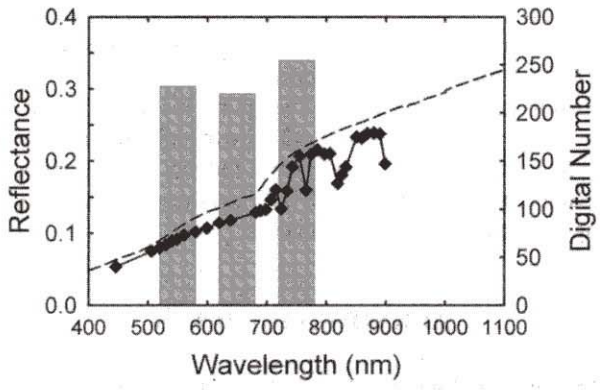

Fig. 15–4. Comparison of reflectances and digital numbers of bare soil at the calibration plot. The dashed line is the measured reflectances using a spectroradiometer, the diamonds are the reflectances from the AISA sensor, and the histogram bars are the digital numbers of the scanned color-infrared photographic transparency obtained using the RCMA.

looking towards the horizon. Qualitative photographic interpretation is not hindered, but quantitative analyses are difficult. Furthermore, canopy anisotropy strongly affects vegetation indices (Walter-Shea et al., 1997). In theory, the NDVI for the two images (Plate 15–4) should be equal; part of the variation in NDVI is explained the effects of canopy anisotropy. The oblique view-angles result in a longer pathlength of light through the canopy, which allows much more absorption of red wavelengths and more reflectance of near-infrared wavelengths by the canopy, thereby increasing NDVI. These problems could be resolved using a lens with longer focal lengths, for example 75 mm, but then the ground area covered by the image would be small, and the image would be much harder to register to a map.

Another common problem of comparing one remotely sensed image with another is the resulting low coefficient of determination (R^2). This is caused by, in part, the errors associated with registering pixel data to a map (Peleg & Anderson, 2002). In one study, the R^2 almost doubled with advanced mathematical techniques of spatial data filtering (Peleg & Anderson, 2002). Therefore, the R^2 values in this study were not an indication that RCMA imagery lacks promise for agricultural remote sensing.

Vegetation indices such as MCARI are designed to measure the chlorophyll absorption feature, whereas NDVI and some other vegetation indices are related more to plant cover or density (Daughtry et al., 2000). Early reports of NDVI being related to leaf area index (Peterson et al., 1987) were, in retrospect, probably caused by correlations between leaf area index and cover (Myneni & Williams, 1994). Thus, when both cover and nutrient status are variable within a field, use of one type of vegetation index is insufficient to detect problems of both low cover and nutrient deficiency.

The spectral and radiometric resolution of the color-infrared film in the automatic camera used in this study may be the most important limitation for the use of RCMA in other applications of remote sensing. The film was overexposed and the green band did not correlate with calibration data (Fig. 15–4). Blackmer et al. (1996) and Scharf and Lory (2002) flew in regular aircraft and acquired color photographs; they showed that it is possible to detect areas of low nutrient status using green and red bands. With continued advances in the development of digital cameras, it will be technologically feasible to have lightweight digital cameras with four or five channels from the green to near infrared.

In conclusion, the high spatial and temporal resolution of RCMA color-infrared imagery can be used to assess overall growth and cover and the low cost may offset some of the limitations discussed above. Indeed, it was surprising to see how well RCMA imagery performed, yet with only preliminary data, caution is required against making exaggerated claims of success.

ACKNOWLEDGMENTS

We thank Jonathan Baker for maintaining and piloting the model aircraft and John Schroeder and the students of Imagine Excellence/El Ingeniero for collecting the field data. Also, we thank: Patrick Coronado, Charles Buffalano, and Robert Savage of NASA Goddard Space Flight Center and the Academy of Model Aeronau-

tics Goddard Model Aircraft Club for discussions about model aircraft and providing the initial pilots. Finally, we thank Shunlin Liang of the University of Maryland for the AISA data, and Dan Shirley and the BARC Farm Operations Branch for field cultivation.

REFERENCES

Blackmer, T.M, J.S. Schepers, G.E. Varvel, and G.E. Meyer. 1996. Analysis of aerial photography for nitrogen stress within corn fields. Agron. J. 88:729-733.

Daughtry, C.S.T., C.L. Walthall, M.S. Kim, E. Brown de Colstoun, and J.E. McMurtrey III. 2000. Estimating corn leaf chlorophyll concentration from leaf and canopy reflectance. Remote Sens. Environ. 74:229-239.

Kim, M.S. 1994. The use of narrow spectral bands for improving remote sensing estimation of fractionally absorbed photosynthetically active radiation (f_{APAR}). M.S. thesis. Department of Geography, University of Maryland, College Park.

Lu, Y.-C., C. Daughtry, G. Hart, and B. Watkins. 1997. The current state of precision farming. Food. Rev. Int. 13(2):141–162.

Moran, M.S., Y. Inoue, and E.M. Barnes. 1997. Opportunities and limitations for image-based remote sensing in precision crop management. Remote Sens. Environ. 61:319–346.

Myneni, R.B., and D.L. Williams. 1994. On the relationship between FAPAR and NDVI. Remote Sens. Environ. 49:200–211.

Peleg, K., and G.L. Anderson. 2002. FFT regression and cross-noise reduction for comparing images in remote sensing. Int. J. Remote Sens. 23:2097–2124.

Peterson, D.L., M.A. Spanner, S.W. Running, and K.B. Tueber. 1987. Relationship of thematic mapper simulator data to leaf area index of temperate coniferous forests. Remote Sens. Environ. 22:323–341.

Pierce, F.J., and P. Nowak. 1999. Aspects of precision agriculture. Adv. Agron. 67:1–85.

Ritchie, S.W., J.J. Hanson, and G.O. Benson. 1993. How a corn plant develops. Special Report no. 48. Iowa State University of Science and Technology, Cooperative Extension Service, Ames.

Quilter, M.C., and V.J. Anderson. 2000. Low altitude/large scale aerial photographs: A tool for range and resource managers. Rangelands 22(2):13–17.

Scharf, P.C., and J.A. Lory. 2002. Calibrating corn color from aerial photographs to predict sidedress nitrogen need. Agron. J. 94:397–404.

Walter-Shea, E.A., J. Privette, D. Cornell, M.A. Mesarch, and C.J. Hays. 1997. Relations between directional spectral vegetation indices and leaf area and absorbed radiation in alfalfa. Remote Sens. Environ. 6:162–177.

Walthall, C.L., J.-L. Roujean, and J. Morisette. 2000. Field and landscape BRDF optical wavelength measurements: Experience, techniques, and the future. Remote Sens. Rev. 18:503–531.

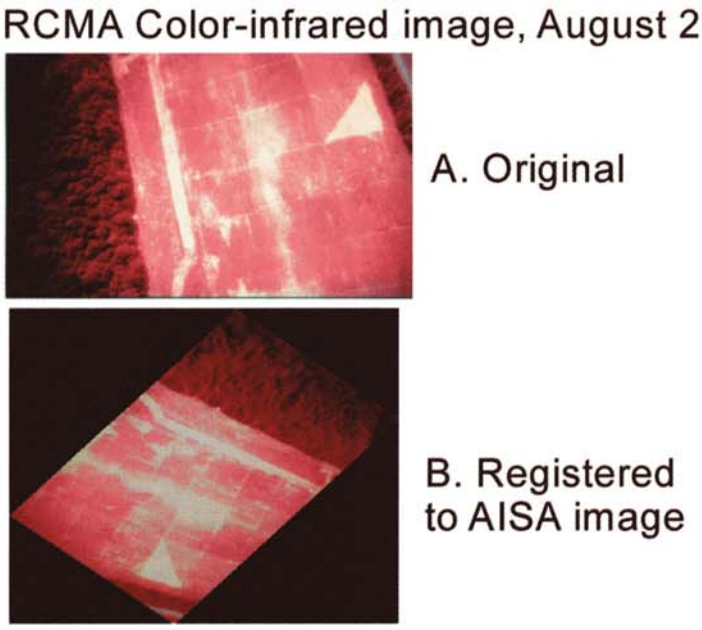

Plate 15–3. RCMA color-infrared image acquired over corn on August 29, 2001. A. Scanned photographic transparency, B. Registered image.

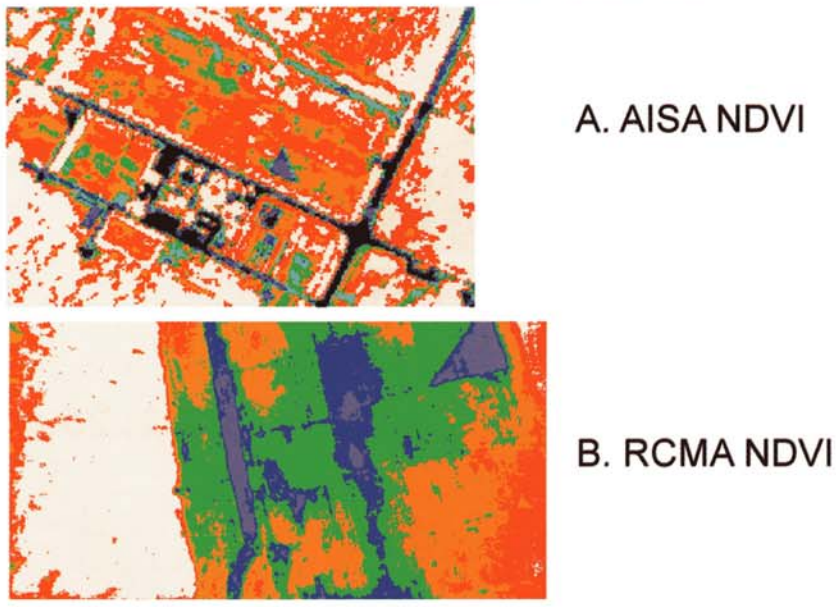

Plate15–4. NDVI from A. AISA (August 22, 2001) and B. RCMA (August 29, 2001). Colors represent different intervals of NDVI: black < 0.0, purple 0.0–0.25, blue 0.25–0.35, green 0.35–0.45, orange 0.45–0.55, red 0.55–0.65, and white > 0.65.

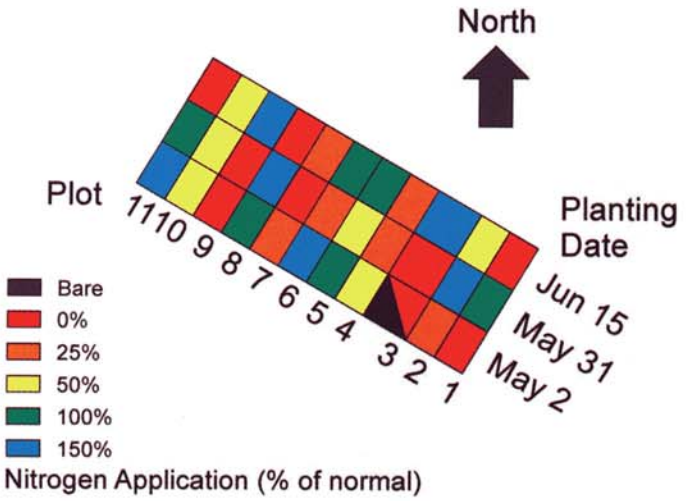

Plate 15–1. Experimental design with different planting dates and levels of applied nitrogen in corn. The 100% rate of applied nitrogen is 145 kg N/ha, with 20 kg N/ha starter nitrogen applied to all plots. Different planting dates allow different sizes of corn to be remotely sensed on one date. The bare area in plot 3 for the early planting date had a very low initial density of corn seedlings, and therefore was maintained as bare soil for image calibration.

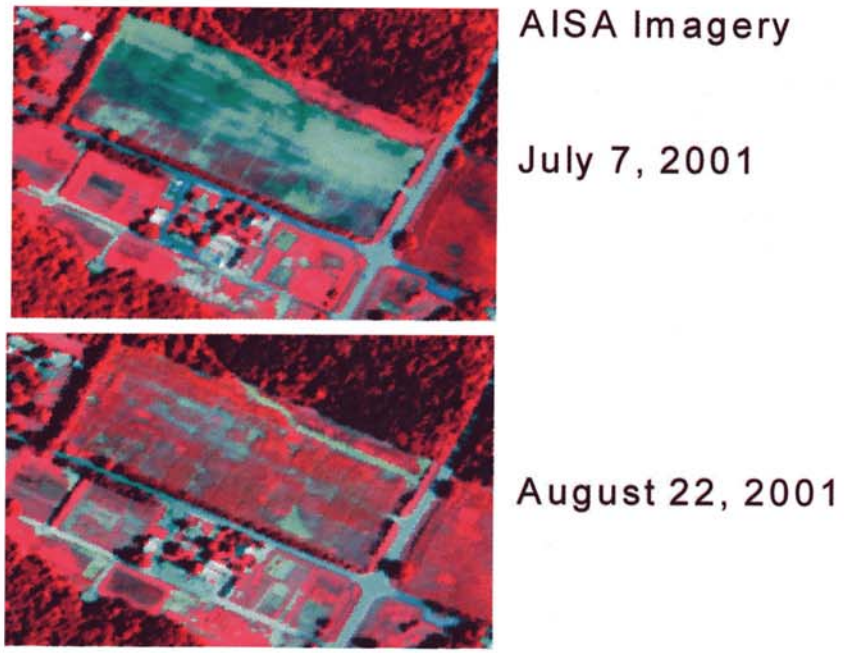

Plate 15–2. AISA color-infrared image of the corn experiment, A. July 7, 2001, and B. August 22, 2001. The near-infrared channel is displayed as red, the red channel is displayed as green, and the green channel is displayed as blue, so areas that are white have high reflectances in the near-infrared, red and green.